Automated projection spectroscopy (APSY)

Supplementary Material

Sebastian Hiller, Francesco Fiorito, Kurt Wüthrich and Gerhard Wider

Institut für Molekularbiologie und Biophysik

Eidgenössische Technische Hochschule Zürich (ETH)

CH-8093 Zürich, Switzerland

Experimental schemes for APSY NMR

The pulse sequence for the 4D APSY-HNCOCA experiment (Fig. 6) was derived from the pulse sequence for 3D HN(CO)CA (1) by adding an evolution period for ^{13}C', similar to 4D TROSY-HNCOCA (2). At a ^{1}H frequency of 750 MHz, the three indirect dimensions ω_1(^{15}N), ω_2(^{13}C') and ω_3(^{13}C$^{\alpha}$) were recorded with spectral widths of 1600 Hz, 1900 Hz and 5700 Hz, respectively, and projected onto one indirect dimension using two projection angles α and β (Table 1). The interscan delay was 1s, and 8 transients were accumulated per data point in the indirect dimension. 1024 complex points were recorded in the direct dimension, with a sweep width of 11.0 ppm. Prior to Fourier transformation, the FID was multiplied with a 75°-shifted sine bell (3) and zero-filled to 2048 complex points. In the indirect dimension, the data was multiplied with a 75°-shifted sine bell and zero-filled to the nearest-next power of 2 complex points before Fourier transformation (4). The spectra were phased automatically using PROSA (5). The baseline was corrected using the IFLAT method (6) in the direct dimension and polynomials in the indirect dimension. j = 27 projections were recorded with the following projection angles α and β, and numbers of complex points in the indirect dimension, n: (α, β, n) = (0°, 0°, 48), (0°, 90°, 42), (90°, 0°, 16), (±30°, 0°, 54), (±60°, 0°, 44), (0°, ±30°, 48), (0°, ±60°, 64), (90°, ±30°, 24), (90°, ±60°, 40), (±30°, ±30°, 56), (±60°, ±30°, 56), (±45°, ±60°, 64).

In the 5D APSY-HACACONH experiment, the pulse sequence of Kim and Szyperski (7) was modified to suppress magnetization pathways starting on glycine H$^{\alpha}$ (8) (Fig. 7). (Magnetization transfers starting at glycines produce pairs of peaks for which 4 of the 5 chemical shifts are identical, differing only in the H$^{\alpha}$-shift. Such pairs of peaks are close in the multidimensional space. In principle, APSY could cope with this situation.) At a ^{1}H frequency of 500 MHz, the four indirect dimensions ω_1(^{1}H$^{\alpha}$), ω_2(^{13}C$^{\alpha}$), ω_3(^{13}C'), and ω_4(^{15}N) were measured with spectral widths of 2000 Hz, 3600 Hz, 1600 Hz and 1550 Hz, respectively, and projected onto one indirect dimension using three projection angles α, β and γ (Table 1). In total, 28 projections were recorded with 128 complex points in the indirect dimension, using the parameters given in Table 2. The 28 projection spectra are shown in Fig. 9. The interscan delay was 1s, and 4 transients were accumulated per data point in the indirect dimension. 1024 complex points were recorded in the direct dimension with a spectral width of 12.0 ppm. The projection spectra were processed in the same way as described above for the 4D APSY-HNCOCA experiment.

Figures Supplementary Material

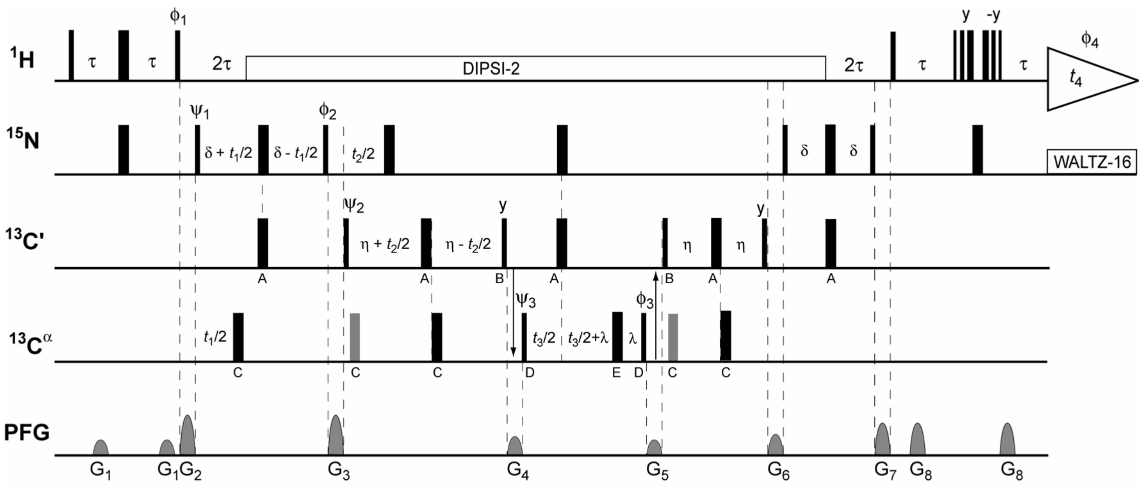

Figure 6. Pulse sequence used for 4D APSY-HNCOCA. Radio-frequency pulses were applied at 118.0 ppm for ^{15}N, at 174.0 ppm for ^{13}C', at 56.0 ppm for ^{13}C$^{\alpha}$, and at 4.7 ppm for ^{1}H. The carrier frequency on the carbon channel was switched between the ^{13}C' and ^{13}C$^{\alpha}$ carrier positions where indicated by the two vertical arrows. Narrow and wide bars represent 90° and 180° pulses, respectively. Pulses marked with an upper case letter were applied as shaped pulses; A: Gaussian shape, duration 100µs; B: Gaussian shape, 120µs; C: I-burp (9), 200µs; D: Gaussian shape, 80µs; E: RE-burp (9), 350µs (durations depend on the spectrometer frequency, here 750 MHz). All other pulses were rectangular pulses applied with high power. The last six ^{1}H pulses represent a 3-9-19 WATERGATE element (10). Grey ^{13}C$^{\alpha}$-pulses were applied to compensate for off-resonance effects of selective pulses (11). Decoupling using DIPSI-2 (12) on ^{1}H and WALTZ-16 (13) on ^{15}N is indicated by rectangles. t_4 is the acquisition period. On the line marked PFG, curved shapes indicate sine bell-shaped pulsed magnetic field gradients applied along the z-axis, with the following durations and strengths: G_1, 700 µs, 13 G/cm; G_2, 1000 µs, 35 G/cm; G_3, 1000 µs, 35 G/cm; G_4, 800 µs, 16 G/cm; G_5, 800 µs, 13 G/cm; G_6, 800 µs, 18 G/cm; G_7, 1000 µs, 28 G/cm; G_8, 1000 µs, 28 G/cm. Phase cycling: $\phi_1 = \{y, -y\}$ $\phi_2 = \{x, x, -x, -x\}$, $\phi_3 = \{4\ x, 4\ -x\}$, $\phi_4 = \{x, -x, -x, x, -x, x, x, -x\}$, all other pulses = x. The following delays were used: τ = 2.7 ms, δ = 13.75 ms, η = 4.5 ms, λ = 200 µs. The indirect evolution times $t_1 - t_3$ were incremented according to the projections angles α and β (see text and Table 1). Quadrature detection for the indirect dimensions was achieved using the hypercomplex Fourier transformation method for projections (14), with the phases ψ_1–ψ_3.

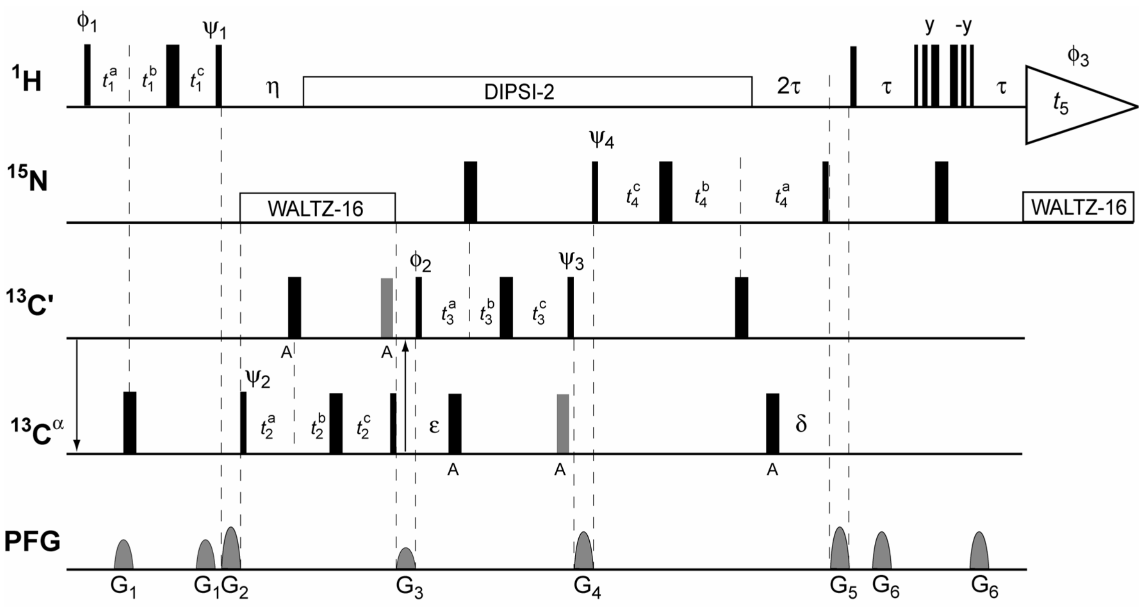

Figure 7. Pulse sequence used for the 5D APSY-HACACONH experiment. Radio-frequency pulses were applied at 4.7 ppm for ^1H, at 118.0 ppm for ^{15}N, at 173.0 ppm for $^{13}C'$ and at 54 ppm for $^{13}C^{\alpha}$. Narrow and wide bars represent 90º and 180º pulses, respectively. Pulses marked "A" were applied as Gaussian shapes, with 120 μs duration at a ^1H frequency of 500 MHz. All other pulses on $^{13}C^{\alpha}$ and $^{13}C'$ had rectangular shape, with a duration of $\sqrt{3}/\left(\Delta\omega\left(C^{\alpha},C'\right)\cdot 2\right)$ and $\sqrt{15}/\left(\Delta\omega\left(C^{\alpha},C'\right)\cdot 4\right)$ for 90º and 180º pulses, respectively. Pulses on ^1H and ^{15}N were applied with rectangular shape and high power. The last six ^1H pulses represent a 3-9-19 WATERGATE element (10). Grey pulses on $^{13}C'$ and $^{13}C^{\alpha}$ were applied to compensate for off-resonance effects of selective pulses (11). Decoupling using DIPSI-2 (12) on ^1H and WALTZ-16 (13) on ^{15}N is indicated by rectangles. t_5 represents the acquisition period. On the line marked PFG, curved shapes indicate sine bell-shaped pulsed magnetic field gradients applied along the z-axis with the following durations and strengths: G_1, 800 μs, 18 G/cm; G_2, 800 μs, 26 G/cm; G_3, 800 μs, 13 G/cm; G_4, 800 μs, 23 G/cm; G_5, 800 μs, 26 G/cm; G_6, 800 μs, 23 G/cm. Phase cycling: ϕ_1 = {x, x, –x, –x} ϕ_2 = {x, –x}, ϕ_3 = {x, –x, –x, x}, ψ_1 = y, all other pulses = x. The following initial delays were used: $t_1^a = t_1^c = 1.9\,ms$, $t_1^b = 0\,ms$, $t_2^a = 4.7\,ms$, $t_2^b = 8.8\,ms$, $t_2^c = 13.5\,ms$, $t_3^a = t_3^c = 11.0\,ms$, $t_3^b = 0\,ms$, $t_4^a = t_4^c = 11.0\,ms$, $t_4^b = 0\,ms$. The delays τ = 2.7 ms and η = 3.6 ms were fixed, and the delays δ and ε were adjusted to $\delta = \left(t_4^a + t_4^b - t_4^c\right)/2$ and $\varepsilon = 4.7ms + \left(t_3^a + t_3^b - t_3^c\right)/2$ during the experiment. In the indirect four dimensions, constant-time or semi-constant time evolution

periods were applied, depending on the increment for the dimension resulting from the chosen projection angles α, β and γ (Table 2). Quadrature detection for the indirect dimensions was achieved using the hypercomplex Fourier transformation method for projections (14) with the phases ψ_1, ψ_2, ψ_3 and ψ_4 (ψ_1, ψ_2 and ψ_3 were incremented and ψ_4 was decremented in 90° steps).

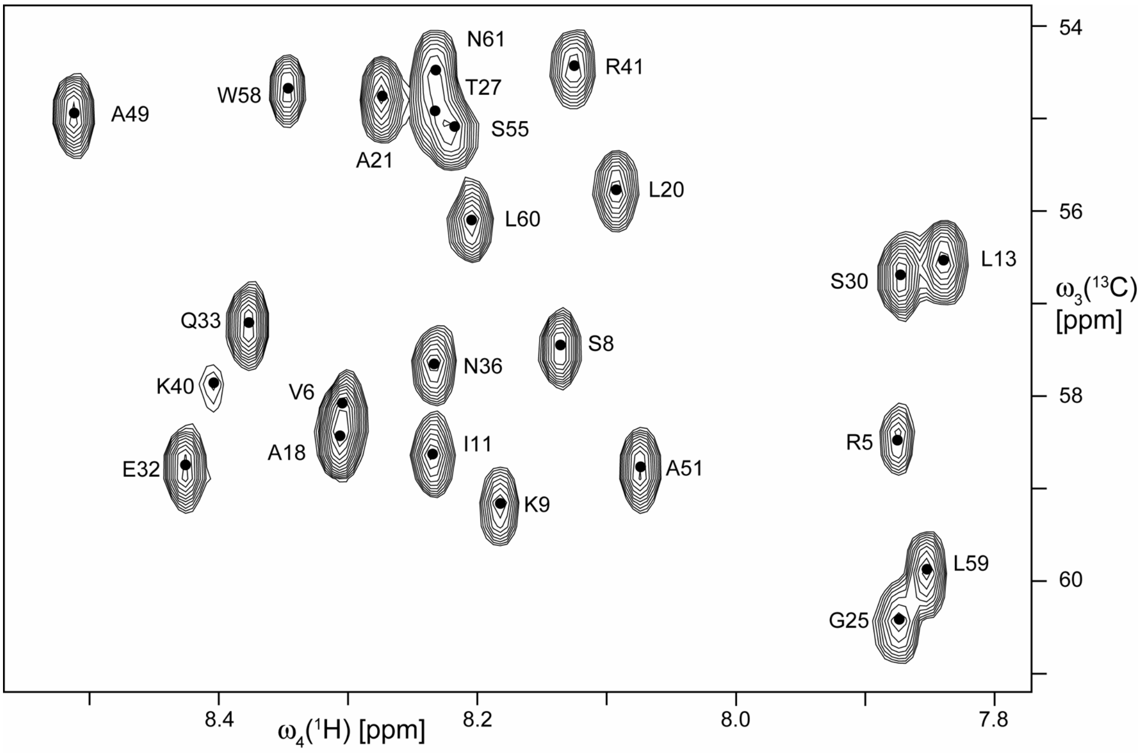

Figure 8. Region of a 4D APSY-HNCOCA spectrum of 434-repressor(1–63) measured with the experimental scheme shown in Fig. 6. The projection was recorded with the angles $\alpha = 0°$ and $\beta = 90°$, which corresponds to a ($H^{N(i)}$, $C^{\alpha(i-1)}$) correlation spectrum. The spectral region shown contains 24 resonances that were all correctly identified by APSY in the associated 4D space. The black dots indicate the peak coordinates from the final 4D APSY peak list. The assignment of the resonances is given using the one-letter amino acid code and the sequence number of the amide proton.

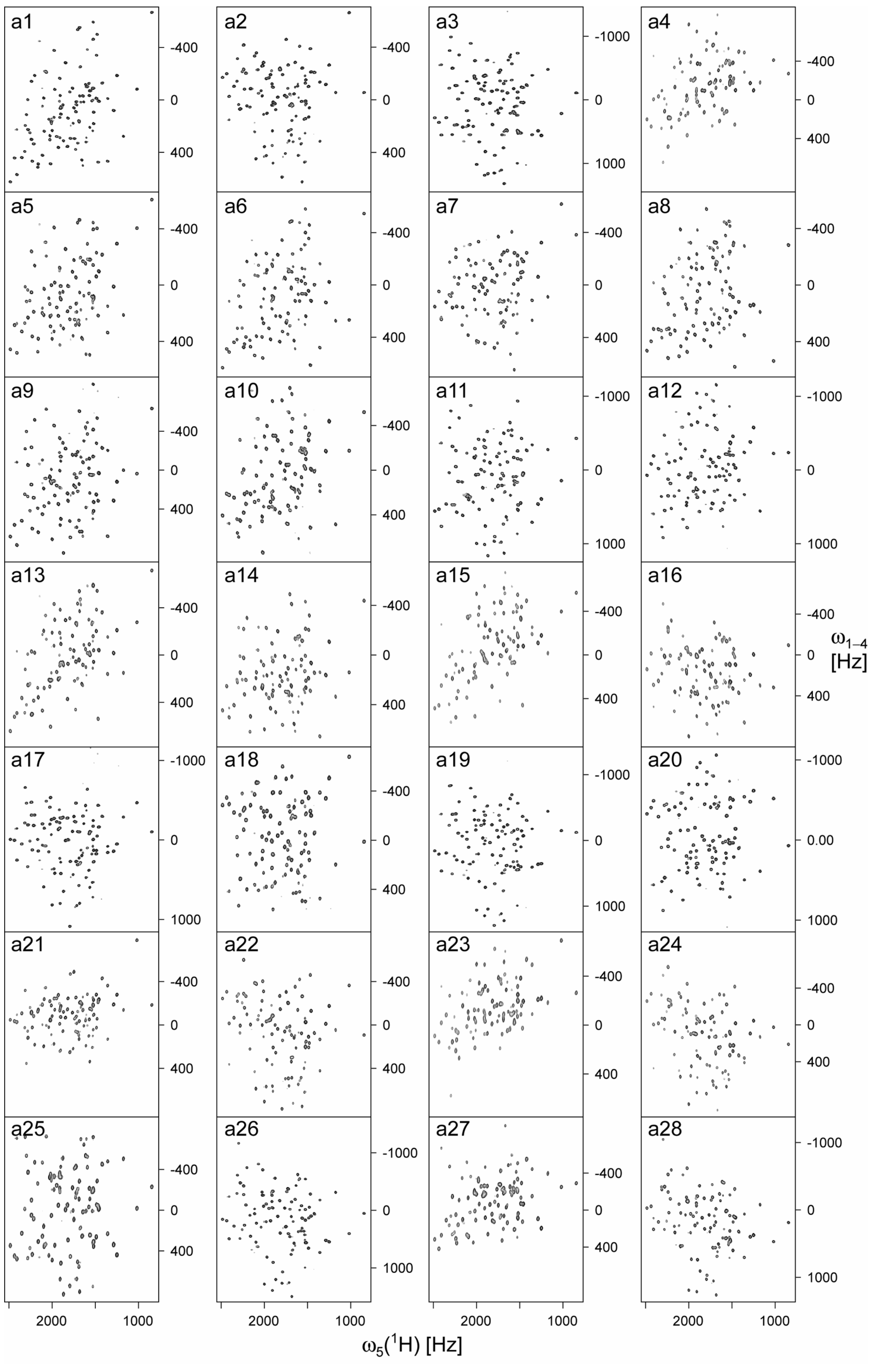
a1
a2
a3
a4
a5
a6
a7
a8
a9
a10
a11
a12
a13
a14
a15
a16
a17
a18
a19
a20
a21
a22
a23
a24
a25
a26
a27
a28
-1000
-400
0
400
1000
0.00
2000
1000
ω_{1-4} [Hz]
$\omega_5(^1H)$ [Hz]

Figure 9. 28 2D projections a1 to a28 of the 5D-APSY-HACACONH experiment measured using the scheme of Fig. 7 with the protein TM1290 on a 500 MHz spectrometer equipped with a z-gradient triple resonance cryogenic probehead. The dimension $\omega_{1\text{–}4}$ is the projection of the four indirect dimensions ω_1(^{1}H$^{\alpha}$), ω_2(^{13}C$^{\alpha}$), ω_3(^{13}C'), and ω_4(^{15}N) obtained with the projection angles α, β and γ (Tables 1 and 2). The scales are centered on the carrier frequencies of 118.0 ppm for ^{15}N, 173.0 ppm for ^{13}C', 54.0 ppm for ^{13}C$^{\alpha}$, and 4.7 ppm for ^{1}H. The projection angles and the spectral widths in the projected indirect dimension are given in Table 2. All projections are plotted with identical contour parameters.

Tables Supplementary Material

Table 2. Projection angles and spectral widths (*SW*)[a] in the dimension ω_{1-4}[b] used for recording the 28 2D projection spectra a1–a28 shown in Figure 9.

	α	β	γ	*SW* [Hz]
a1	0º	0º	0º	1550
a2	90º	0º	0º	1600
a3	0º	90º	0º	3600
a4	0º	0º	90º	2000
a5	30º	0º	0º	2142
a6	-30º	0º	0º	2142
a7	60º	0º	0º	2161
a8	-60º	0º	0º	2161
a9	0º	30º	0º	3142
a10	0º	-30º	0º	3142
a11	0º	60º	0º	3893
a12	0º	-60º	0º	3893
a13	0º	0º	30º	2342
a14	0º	0º	-30º	2342
a15	0º	0º	60º	2507
a16	0º	0º	-60º	2507
a17	90º	30º	0º	3186
a18	90º	-30º	0º	3186
a19	90º	60º	0º	3918
a20	90º	-60º	0º	3918
a21	90º	0º	30º	2386
a22	90º	0º	-30º	2386
a23	90º	0º	60º	2532
a24	90º	0º	-60º	2532
a25	0º	90º	30º	4118
a26	0º	90º	-30º	4118
a27	0º	90º	60º	3532
a28	0º	90º	-60º	3532

[a] The spectral width SW in the projected indirect dimensions is calculated from $SW = \sum_{z=1}^{4} \mathrm{p}_1^z \cdot SW_z$, where the p_1^z s are the coordinates of the unit vector $\vec{\mathrm{p}}_1$ (Eq. (1)) and the SW_z are the spectral widths of the individual four indirect dimensions.

[b] The dimension ω_{1-4} is the projection of the four indirect dimensions $\omega_1(^1H^\alpha)$, $\omega_2(^{13}C^\alpha)$, $\omega_3(^{13}C')$ and ω_4 (^{15}N) with the projection angles α, β and γ (Tables 1 and 2).

Table 3. Data base of proteins used to generate the Figure 5. In addition to these 53 proteins, the chemical shifts of 434-repressor(1–63) (BMRB data 2539 and unpublished data) were used.

BMRB number	number of residues
4070	205
4093	138
4188	138
4193	214
4198	161
4215	136
4288	105
4384	262
4572	75
4575	211
4599	161
4671	159
4679	165
4881	179
4913	115
4938	132
4959	148
5013	120
5177	166
5308	107
547	148
5540	148
5557	170
5598	102
5629	111
5761	119
5884	138

5928	140
5976	103
6125	228
6133	116
6236	117
6295	251
5560	116
4101	214
4267	179
4282	183
4321	166
4376	185
4848	240
4854	240
5054	165
5232	199
5316	288
5398	187
5483	187
5627	282
5668	187
5756	184
5823	242
6202	215
6241	182

References Supplementary Material

1. Grzesiek, S. & Bax, A. (1992) *J. Magn. Reson.* **96**, 432–440.
2. Yang, D. W. & Kay, L. E. (1999) *J. Am. Chem. Soc.* **121**, 2571–2575.
3. De Marco, A. & Wüthrich, K. (1976) *J. Magn. Reson.* **24**, 201–204.
4. Bartholdi, E. & Ernst, R. R. (1973) *J. Magn. Reson.* **11**, 9–19.
5. Güntert, P., Dötsch, V., Wider, G. & Wüthrich, K. (1992) *J. Biomol. NMR* **2**, 619–629.
6. Bartels, C., Güntert, P. & Wüthrich, K. (1995) *J. Magn. Reson.* **A117**, 330–333.
7. Kim, S. & Szyperski, T. (2003) *J. Am. Chem. Soc.* **125**, 1385–1393.
8. Burum, D. P. & Ernst, R. R. (1980) *J. Magn. Reson.* **39**, 163–168.
9. Geen, H. & Freeman, R. (1991) *J. Magn. Reson.* **93**, 93–141.
10. Sklenar, V., Piotto, M., Leppik, R. & Saudek, V. (1993) *J. Magn. Reson.* **A102**, 241–245.
11. McCoy, M. A. & Müller, L. (1992) *J. Magn. Reson.* **99**, 18–36.
12. Shaka, A. J., Lee, C. J. & Pines, A. (1988) *J. Magn. Reson.* **77**, 274–293.
13. Shaka, A. J., Keeler, J., Frenkiel, T. & Freeman, R. (1983) *J. Magn. Reson.* **52**, 335–338.
14. Kupce, E. & Freeman, R. (2004) *J. Am. Chem. Soc.* **126**, 6429–6440.